Aquaculture 602 (2025) 742347

Contents lists available at ScienceDirect

Aquaculture

journal homepage: www.elsevier.com/locate/aquaculture

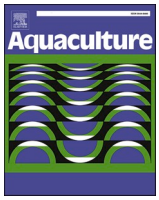

Triploidy induction through *cntd1* knockout in red crucian carp (*Carassius auratus* red var.)

Huilin Li [1], Yu Zhang [1], Lina Zhang, Juan Li, Yuan Ou, Ming Wen, Zehong Wei, Jing Wang, Yu Deng, Yinjun Jiang, Conghui Yang, Yuqin Shu [*], Shaojun Liu [*]

Engineering Research Center of Polyploid Fish Reproduction and Breeding of the State Education Ministry, College of Life Sciences, Hunan Normal University, Changsha 410081, Hunan, People's Republic of China

ARTICLE INFO

Keywords:
cntd1
Knockout
Triploid
Triploidy
Polyploid breeding

ABSTRACT

Triploid fish are distinguished by their rapid growth rate, enhanced resistance, and bisexual sterility, making them highly desirable for breeding purposes. A recent innovation in triploid production involves the utilization of *cntd1* (*cyclin N-terminal domain containing 1*) knockout in zebrafish. In this study, this method was successfully applied to red crucian carp (RCC) through the implementation of the clustered regularly interspaced short palindromic repeats/CRISPR-associated endonuclease 9 (CRISPR/Cas9) technique. Analysis of the *cntd1* knockout F0 generation in RCC revealed phenotypes similar to those observed in Cntd1-deficient zebrafish. The male F0 RCC exhibited severely inhibited spermatogenesis characterized by pink testes and watery semen. Subsequent examination indicated markedly reduced spermatozoa production, with numerous spermatocytes arrested at the metaphase of meiosis and enriched apoptotic signals in the testes. In contrast, females of the F0 generation spawn normally, but their offspring displayed developmental deformities and variable ploidy levels during embryogenesis. Upon maturation, the offspring were categorized into diploids and triploids based on DNA fluorescence values per cell and chromosome numbers. As previously reported, the erythrocytes of triploids displayed karyorrhexis and dumbbell-shaped nuclei. The current study demonstrates that the method of ploidy regulation based on *cntd1* knockout is adaptive to various species of fish and holds great potential for use in polyploid breeding.

1. Introduction

Polyploid breeding in fish was initiated during the 1950s, marked by the successful acquisition of triploid threespine sticklebacks that reached adulthood in 1959 (Swarup, 1959a, 1959b). Subsequent investigations have consistently demonstrated that triploid fish exhibit growth advantages (Afroz et al., 2021; Chen et al., 2009; Huang et al., 2023; Oppedal et al., 2003; Ren et al., 2022) and heightened resistance (Liu et al., 2018; Liu et al., 2021b), in addition to exhibiting bisexual sterility (Benfey, 2016). The sterility attribute serves to prevent farmed fish from intermingling with natural aquatic habitats for reproductive purposes, thereby fostering the conservation of indigenous germplasm resources (Cotter et al., 2000). In China, more than 105 nonnative fish species have escaped into natural aquatic habitats, 61 of which have established viable populations in the wild, posing a significant ecological threat to local aquatic ecosystems (Ju et al., 2020). Consequently, the pursuit of sustainable aquaculture practices requires the production of sterile fish incapable of reproducing with wild stocks after escape, thereby mitigating the environmental impact (Güralp et al., 2020; Wargelius et al., 2016; Yang et al., 2022). Currently, triploidization is a dominant and pragmatic strategy for inducing sterility in aquaculture (Arai, 2001; Benfey, 2001, 2016; Cotter et al., 2000; Wong and Zohar, 2015).

However, the widespread adoption of triploid fishes is severely limited by the current methods used to produce them. Triploid fish are efficiently generated by disrupting the extrusion of the second polar body via temperature and hydrostatic shock (Carrasco et al., 1998; Chourrout et al., 1986; Felip et al., 2001; Goo et al., 2015; Káldy and Patakiné Várkonyi, 2021; Lahnsteiner and Kletzl, 2018; Nwachi and Esa, 2016; Piferrer et al., 2009). Nonetheless, artificial induction methods typically lead to higher rates of malformation and reduced hatching and survival rates, with surviving embryos often exhibiting partial triploidy

* Corresponding authors at: College of Life Sciences, Hunan Normal University, #36 Lushan South Road, Changsha 410081, PR China.
E-mail addresses: shuyuqin@hunnu.edu.cn (Y. Shu), lsj@hunnu.edu.cn (S. Liu).
[1] These authors contributed equally to this work and should be considered co-first authors.

https://doi.org/10.1016/j.aquaculture.2025.742347
Received 17 August 2024; Received in revised form 20 February 2025; Accepted 21 February 2025
Available online 23 February 2025

(Hassan et al., 2018; Nwachi and Esa, 2016), which poses challenges for large-scale production. Consequently, the primary challenge lies in acquiring bisexual-fertile tetraploids. Researchers have attempted to achieve this by inhibiting the first or second egg cleavage in nearly a dozen fish species, such as rainbow trout, medaka, and turbot. Despite the successful production of tetraploidized embryos, the transition to tetraploid adults has proven difficult, and achieving tetraploid fertility via this approach is notably challenging (Baars et al., 2016; Lebeda and Flajshans, 2015; Martins et al., 2021; Nam et al., 2004; Peruzzi and Chatain, 2003; Zhu et al., 2017).

In our previous study, a novel approach for tetraploidization was established by disrupting the *cntd1* gene in zebrafish model (Ou et al., 2024). Similar to studies in nematodes and mice (Holloway et al., 2014; Yokoo et al., 2012), zebrafish Cntd1 was found to play a role in the formation of meiotic crossovers, with its disruption leading to a reduced frequency of crossovers (Ou et al., 2024). Interestingly, the zebrafish model further revealed that the defect of crossover formation led to the random segregation of homologous chromosomes during meiosis, thereby enabling Cntd1-deficient females to produce partial chromosome-unreduced eggs, as well as triploid and tetraploid offspring. In contrast, tetraploid heterozygotes, which possess a functional allele of *cntd1*, underwent normal meiotic progression and produced reduced diploid gametes. Mating of tetraploid heterozygotes with diploids resulted in all-triploid progeny (Ou et al., 2024).

In the present study, we employed CRISPR/Cas9 technology to disrupt the *cntd1* gene in RCC, resulting in mutations in a subset of germ cells within the F0 generation. Subsequently, triploid RCCs were identified within the F1 generation produced by the F0 females. This study provides additional evidence supporting the widespread applicability of gametes manipulation and ploidy regulation facilitated by *cntd1* knockout as a viable strategy.

2. Material and methods

2.1. Cntd1 knockout in RCC

The *cntd1* (Gene ID: 113056560) sequence of RCC was obtained from the NCBI database and confirmed by PCR amplification and sequencing. Two knockout targets (target_1:1179–1196 bp; target_2:1310–1334 bp) were designed on the second and third exons. Primers (F: 1037–1057 bp, R: 1461–1480 bp) for genotyping were designed to flank the targeted region and were used to amplify the fragment encompassing the target region. The gRNA was synthesized utilizing the T7 High Yield RNA Transcription Kit (E131, Novoprotein, China), followed by purification, quantification, and storage at −80 °C. The Cas9 protein was obtained from Suzhou Nearshore Protein Technology Corporation (E365-01 A, Novoprotein, China). Prior to microinjection, the gRNA and Cas9 proteins were combined to achieve final concentrations of 50 and 100 ng/μL, respectively. The mixture was then injected into I-IV cell-stage RCC embryos with a microinjector (Worcester Polytechnic Institute, pv830, USA), with a total of approximately four to five hundred embryos being injected.

2.2. Genotyping

The sequences of the genotyping primers used were as follows: forward primer, TGAGACTATTGCAAGACTGTC; reverse primer, CATACATTGGAGTACAGGTC. Five F0 embryos or one F1 tail fin was placed into a 1.5 mL EP tube. Subsequently, 200 μL of 50 mM NaOH solution was added, and the mixture was digested at 95 °C for 10 min, followed by brief vortexing for 5 s. After an additional 5 min of digestion, the samples were removed and allowed to cool to room temperature. Next, 20 μL of 1 M Tris-HCl solution was added and thoroughly mixed to serve as a PCR template. The PCR amplification was carried out with the following steps: denaturation at 95 °C for 30 s, annealing at 56 °C for 30 s, and extension at 72 °C for 30 s, with a total of 32 cycles. The target fragment, measuring 410 bp in length, was then amplified using the genotyping primers. Following amplification, PCR products from injected embryos were sequenced with forward primers to assess knockout efficiency. Moreover, PCR fragments amplified from the tail fins of adult F0 RCC were cloned and inserted into the pMD18-T vector and subsequently sequenced to determine the precise sequence of the target region.

2.3. HE staining

The RCC testes were isolated and cut into small segments, which were subsequently fixed in Bouin's solution overnight and then preserved in 70 % ethanol. The subsequent procedures were as follows: sequential gradient dehydration using 70 %, 80 %, 90 %, 95 %, and 100 % ethanol for 20 min each, with two repetitions for 100 % ethanol. The samples were then treated with ethanol/xylene (1:1) and xylene until the tissues became transparent. The transparent tissues were then subjected to successive dipping wax treatments at various xylene/soft wax ratios (2:1 and 1:1), followed by single treatments with soft wax and hard wax, each lasting 1 h. After adequate dipping wax treatment, the samples were embedded in paraffin wax and sliced into 6 -μm thick sections, which were mounted on clean slides. These sections were deparaffinized overnight in xylene, followed by hydration using a decreasing ethanol gradient (100 %, 95 %, 90 %, 80 %, 70 %). Once hydrated, the sections were stained with hematoxylin and eosin, differentiated, rinsed, dehydrated, restained, dehydrated again, and subjected to transparency processing before being sealed with coverslips. Finally, the prepared sections were observed using a microscope (Leica, Germany).

2.4. TUNEL staining

Three testes each from the control and F0 generations of *cntd1* knockout RCC were isolated and processed as follows: fixed in 4 % polyformaldehyde, embedded in optimal cutting temperature compound (OTC), and sectioned to a thickness of 5 μm. To assess apoptosis signals, TUNEL staining was performed using the In Situ Cell Death Detection Kit, TMR Red (12,156,792,910, Roche). The fixed tissue sections were incubated for 2 h at 37 °C in a reaction mixture containing terminal deoxynucleotidyl transferase (TdT) enzyme, TMR-conjugated dUTP, and reaction buffer. Subsequently, the slides were washed to remove excess staining solution and counterstained with 4′,6-diamidino-2-phenylindole (DAPI) to visualize the cell nuclei. Finally, the apoptotic signals were observed and analyzed under a fluorescence microscope (Leica, Germany).

2.5. Ploidy analysis using flow cytometry

For the embryo analysis to pre-screen positive F0 females, ten embryos from each F0 female were collected and prepared into five samples. For detailed ploidy analysis in F1 embryos, a single embryo was collected as one sample. All the embryos for flow cytometry analysis were collected at 4 days post fertilization (dpf) and placed in 1.5 mL tubes. Following the removal of excess water, a mixture comprising 50 μL of phosphate-buffered saline (PBS) and 50 μL of acid-citrate-dextrose (ACD) was introduced. After sufficient incision with scissors, 300 μL of PBS (1×) was added, followed by 300 μL of DAPI solution at a working concentration, with precautions taken to avoid exposure to light. The resulting mixture was then thoroughly mixed and allowed to incubate for 10 min.

For adult analysis, venous blood was aseptically drawn from the caudal vein of the RCC using a 1 mL sterile syringe. The collected blood was promptly transferred to a 1.5 mL EP tube containing 100 μL of ACD, followed by the addition of 300 μL of DAPI solution. The resulting mixture was then subjected to a 10-min staining process without light.

Before analysis, the prepared sample was filtered through a 30 μm

filter to eliminate residual tissue debris. The obtained filtrate was then assayed using a flow cytometer (PA, Partec, Germany).

2.6. Blood cell culture

For each group, three individuals aged eight months with an average weight of 15.43 g were selected for chromosome preparation. Using a sterile 1 mL syringe, 0.2 mL of 0.1 % sodium heparin solution was aspirated, and subsequently, 0.2 mL of blood was collected from the caudal vein of the RCC, after the caudal peduncle was disinfected with 75 % alcohol to ensure sterility. The blood was immediately sterilized by cauterizing the syringe needle, capping it, and thoroughly mixing it. After this, the syringe was placed needle-side down in a refrigerator at 4 °C for 1 h to facilitate erythrocyte settling. Concurrently, cell culture medium was prepared using RPMI-1640 medium supplemented with 0.001 % sodium heparin, 1.5 % fetal bovine serum, 1 % penicillin–streptomycin solution, and 0.3 mg/mL phytohemagglutinin. After the blood cells settled, the supernatant and interfacial solution were collected and added to 10 mL of the aforementioned culture solution. This composite was then incubated in an environment with 5 % CO_2 at 24 °C. Throughout the incubation period, the culture solution was intermittently agitated every 4–8 h to disperse the blood cells. At the 68-h mark, 50 μL of colchicine (20 μg/mL) was added, and the incubation was halted after an additional 3–4 h.

2.7. Chromosome preparation

The cultured cells were centrifuged at 1000 rpm for 6 min (min) and then resuspended in 10 mL of 0.075 mol/L KCl hypotonic solution. After 30 min of hypotonic treatment at 24 °C, with gentle dispersion every 10 min, 1 mL of a fixative solution (methanol/glacial acetic acid = 3/1) was added for prefixation. Following centrifugation at 900 rpm for 5 min, the cell precipitate was collected. The precipitate was subsequently fixed overnight at 4 °C in 4 mL of fixative solution. After centrifugation at 1000 rpm for 5 min, the precipitate was collected again and subjected to further fixation with 1 mL of fixative solution. The cell suspension was dropped onto precooled slides, immediately passed through an alcohol lamp flame, and air-dried. The dried slides were stained with Giemsa's stain for 35 min, rinsed, and allowed to dry before microscopy. Chromosome photographs were taken using a 100× oil immersion objective.

2.8. Blood smear preparation

For each group, three individuals aged eight months with an average weight of 8.37 g were selected for sample preparation. A 1.5 mL sterile syringe was washed with 0.1 % sodium heparin solution, and then 0.1 mL of blood was drawn from the tail vein of the RCC, which was transferred into an EP tube containing 1 mL of PBS buffer. Subsequently, a drop of the blood sample was deposited 1 cm from the right end of a slide, which was held flat in the left hand. Another slide was used to spread the blood across the first slide at a 45° angle, creating a smear, which was then allowed to air-dry at room temperature. Plenty of Wright's stain solution was applied to completely cover the dried smear and left for three min, followed by the addition of an equal amount of PBS buffer to facilitate mixing with the stain. After standing for 5 min, the slide was washed with running water from the back, dried, and examined under a microscope (DM2500, Leica, Germany) at 100× magnification.

2.9. Statistical analysis

The parameters of erythrocyte sizes were subjected to the independent-samples *t*-test, which were conducted using IBM SPSS Statistics for Windows, version 27.0 (IBMCorp., Armonk, N.Y., USA). The results are presented as mean ± standard error ($n \geq 4$). The results were considered statistically significant at $P < 0.05$.

3. Results

3.1. Knockout of cntd1 in RCC was achieved using the CRISPR/Cas9 system

The designed sequences for the two knockout targets located on the second and third exons of the RCC *cntd1* gene were as follows: target 1_GGGACTGAATCCTGCGGT and target 2_GGCCAAATATATTGAACATCTAATC (Fig. 1A). Following the microinjection of F0 embryos, sequencing was performed with 5′ end primers to detect mutations at the two targeted sites. The detection results showed that the *cntd1* gene in control RCC embryos exhibited a uniform sequence, as indicated by single peaks in the Sanger sequencing results. In contrast, the *cntd1* gene of injected F0 embryos displayed multiple peak sets starting from the first target site, with increased heights of mutant peaks observed at the second target site (Fig. 1B and C), suggesting successful knockout at both target sites. Upon maturation into adult fish, approximately 60–80 F0 RCC remained viable. Subsequently, PCR amplification of the caudal fin genome was conducted, and the PCR fragments containing the targets were cloned and inserted into a vector for sequencing, enabling the acquisition of specific target sequences from the F0 individuals. A comprehensive examination involving 12 female F0 RCC specimens identified 15 mutant sequences, revealing variations such as multilocus mutations, base insertions, or deletions near the target sites (Fig. 1D and E).

3.2. Spermatogenesis was inhibited in the F0 generation of RCC

To investigate the reproductive characteristics of *cntd1* knockout F0 RCC, a total of 27 F0 individuals were examined, of which 12 were identified as males. Notably, in contrast to control RCC males, which typically produce milky-white semen, 9 out of the 12 F0 male individuals examined were found to produce watery semen (Fig. 2A, Movies S1 and S2). The remaining three F0 males exhibited milky-white semen, similar to the control males. Anatomical examination revealed that the testes of the control RCC were milky-white, whereas those of the *cntd1* knockout F0 generation appeared light pink (Fig. 2B). Histological analysis of testes revealed distinct differences in germ cell composition between the two groups: control RCC exhibited plentiful spermatids and mature spermatozoa (Fig. 2C), whereas the *cntd1* knockout F0 generation manifested sparse spermatids and spermatozoa, with numerous spermatocytes arrested at the metaphase of meiosis (Zhang et al., 2021; Ou et al., 2024). These arrested spermatocytes exhibited chromosome clustering in the middle of the bipolar spindle and evident abnormal chromosome segregation (Fig. 2 D). Given the known role of meiotic aberrations in triggering the meiotic checkpoint, resulting in cell cycle arrest and apoptosis, our investigation was extended to assess apoptosis levels during spermatogenesis in both groups of RCC. Remarkably, minimal apoptotic signals were observed in the testes of the control RCC, while an obvious increase in apoptotic signals was detected in the testes of the *cntd1* knockout F0 generation (Fig. 2E and F).

3.3. Embryonic ploidies in F0 female RCC varied from haploid to triploid

In contrast to males, the 15 *cntd1* knockout F0 RCC females identified exhibited normal spawning behavior during the breeding season. To screen for positive F0 females, all F0 RCC females were mated with control males to maximize F1 offspring (Fig. 3A). Flow cytometry analysis revealed that the DNA content per cell of WT RCC embryos was approximately 100 (Fig. 3B), whereas ten out of fifteen F0 females produced embryos with a DNA content of up to 150, indicating the presence of triploids (Fig. 3C-Q). Self-crossing of the control RCC resulted in offspring displaying consistent morphological traits throughout embryonic development, characterized by a straight body axis upon hatching (Fig. 4A-D). Conversely, phenotypic variability was observed among F1 embryos resulting from crosses between *cntd1*

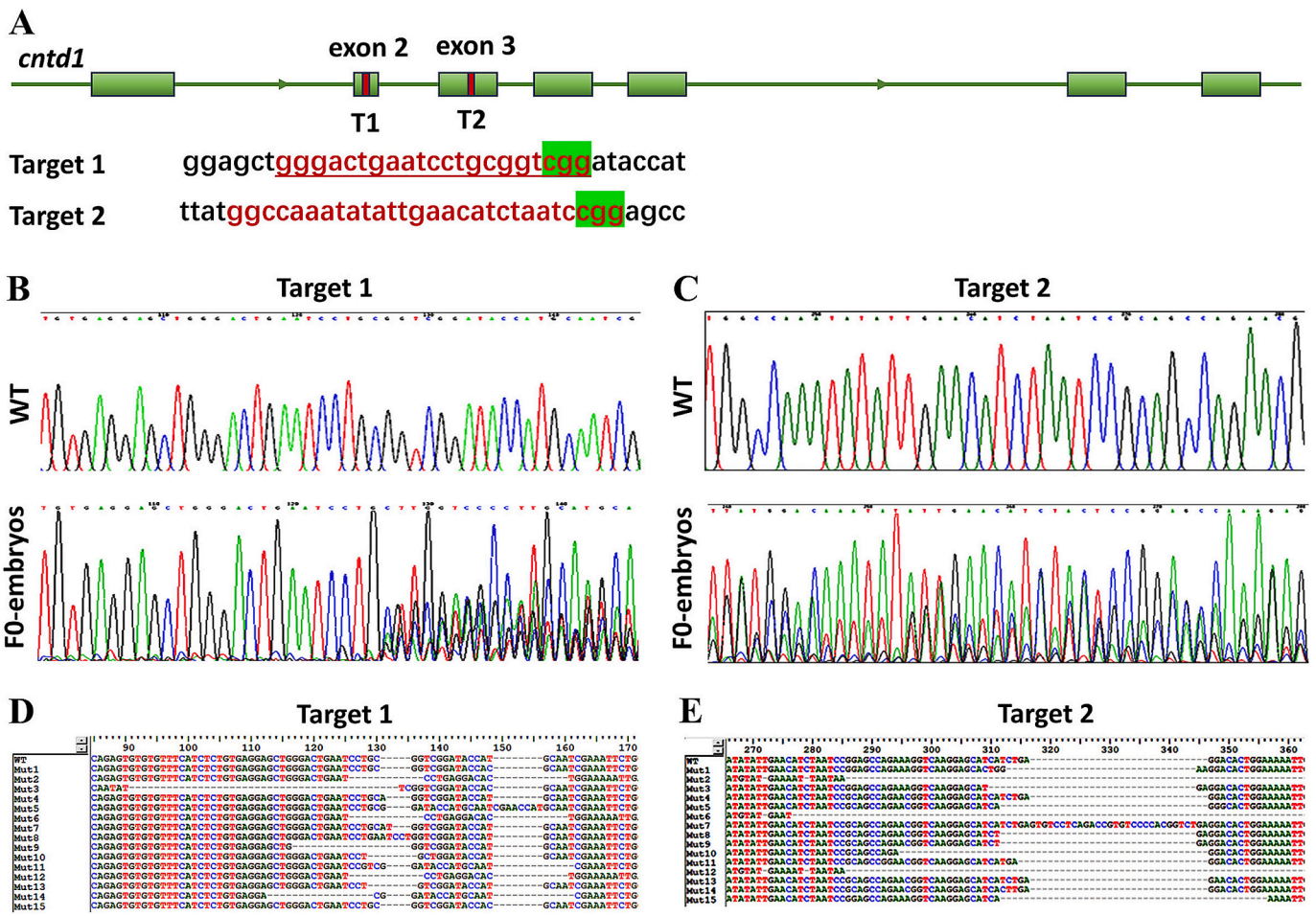

Fig. 1. Effective knockout of *cntd1* in RCC. A, Targets designed on the second and third exons of the RCC *cntd1* gene. The exons and the target region are indicated with green and red boxes, respectively. The target sequence is shown in red, followed by the protospacer-adjacent motif highlighted in green. B, Sanger sequencing maps of target 1 in WT and *cntd1* knockout F0 embryos. C, Sanger sequencing maps of target 2 in WT and *cntd1* knockout F0 embryos. D, BLAST results of the target 1 sequence in WT and *cntd1* knockout F0 adults. E, BLAST results of the target 2 sequence in WT and *cntd1* knockout F0 adults. (For interpretation of the references to colour in this figure legend, the reader is referred to the web version of this article.)

knockout F0 females and control males. While some zygotic embryos from *cntd1* knockout F0 individuals developed similarly to those of controls, those derived from positive F0 females exhibited abnormal development beginning at 24 h post fertilization, showing elevated rates of abnormalities and lethality throughout embryonic development. After hatching, various malformations, such as truncated tails, microcephaly, curvature, and edema, were evident, with affected embryos ultimately succumbing during subsequent development, resulting in the survival of only a subset of zygotes (Fig. 4E-H). Consequently, further analyses were conducted to assess the ploidy of both control embryos and F1 embryos showing aberrant development using flow cytometry. The results revealed that the control embryos were diploid, with single-cell DNA fluorescence values of approximately 100 (Fig. 4I-L). In contrast, F1 embryos encompassed a spectrum of ploidies, including haplodiploids, diploids, triploids, and various aneuploids, as evidenced by single-cell DNA fluorescence values spanning a range of approximately 50 to 150 (Fig. 4M-P).

3.4. Surviving offspring from cntd1 knockout females were diploid and triploid

F1 offspring with deformed embryonic development were raised for 8 months. Subsequently, 35 surviving individuals were randomly selected for flow cytometry analysis. A WT RCC was used as a control, showing a DNA content per cell of approximately 100 (Fig. 5A). Among the F1 offspring, 13 exhibited single-cell DNA content fluorescence values similar to that of WT RCC, while 22 displayed values around 150 (Fig. 5B), suggesting the presence of both diploid and triploid individuals among the surviving offspring. Furthermore, we measured the body weights of these groups and found no significant difference between them, with weights of 9.79 ± 1.36 g and 8.95 ± 0.90 g, respectively (Fig. 5C). Morphologically, individuals from both groups exhibited a range of colors, from grey to gold or red, and displayed similar body shapes and sizes within the same weight range (Fig. 5D-I).

Additionally, three larger individuals from WT RCC and each group of F1 offspring were selected for chromosome analysis (Fig. 6A - C), with corresponding flow cytometry results showing values close to 100, 100 and 150 (Fig. 6D - F). Chromosome preparations from blood cell cultures confirmed that both WT RCC and group 1 of the F1 population possessed 100 chromosomes, whereas group 2 from of the F1 population exhibited 150 chromosomes (Fig. 6G - I), indicating that the surviving F1 offspring were diploid and triploid. Karyotype analysis revealed that WT individuals and the diploid F1 progeny exhibited a karyotype of 22 m + 34 sm + 22 st + 22 t, while the triploid progeny had a karyotype of 33 m + 51 sm + 33 st + 33 t (Fig. 6J - L). Notably, the diploid karyotypes were consistent with previously reported findings (Liu et al., 2001; Qin et al., 2014).

Previous studies have linked polyploid fish with enlarged erythrocytes and aberrant nuclear morphology (Wang et al., 2024; Wang et al., 2020a). Therefore, we further examined the size and morphology of

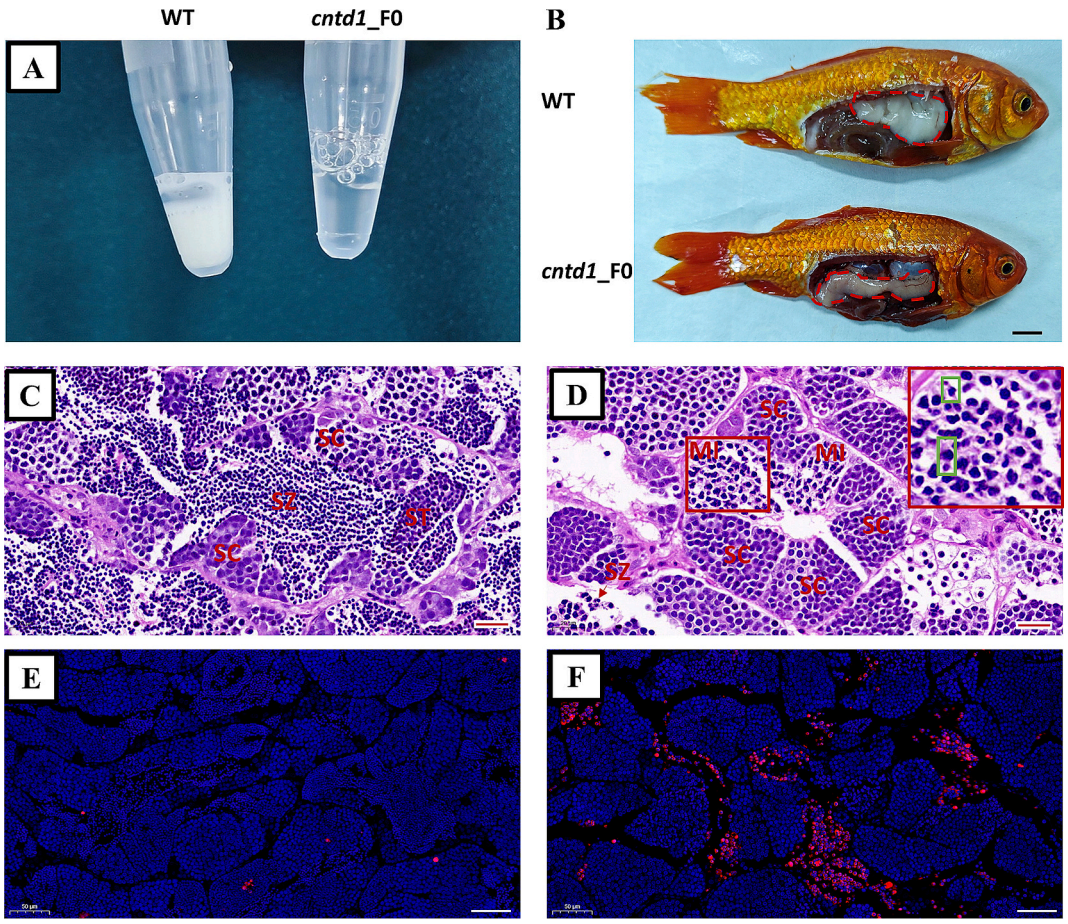

Fig. 2. Inhibited spermatogenesis in *cntd1* knockout F0 RCC. A, Representative view of semen from WT and *cntd1* knockout F0 males. B, Anatomical views of testes from WT and *cntd1* knockout F0 males. The red dotted line indicates the testis. The scale bar represents 1 cm. C and D, Histological analysis of testes from WT (C) and *cntd1* knockout F0 (D) males. SC, Spermatocytes; ST, Spermatids; SZ, Spermatozoa; MI, Metaphase of meiosis I. The magnified region is indicated by a red box. Equatorial-plate chromosomes were indicated by a green box. The scale bar represents 20 μm. E and F, TUNEL staining of testes from rom WT (E) and *cntd1* knockout F0 (F) males. The red spots indicate apoptotic signals. The scale bar represents 50 μm. (For interpretation of the references to colour in this figure legend, the reader is referred to the web version of this article.)

erythrocytes in diploid and triploid F1 offspring. The results showed that the erythrocytes in diploid F1 offspring were consistently oval-shaped and uniform in size, whereas a subset of erythrocytes in triploid F1 offspring exhibited karyorrhexis and dumbbell-shaped nuclei (Fig. 7A-D). Statistical analysis revealed that approximately 7.7 % of the erythrocytes in the triploid F1 offspring displayed aberrant nuclear morphology (Fig. 7E). In addition, the long diameter of erythrocytes in triploid F1 RCC was significantly greater than that in diploid F1 RCC (Fig. 7F).

4. Discussion

In this study, we employed CRISPR/Cas9 technology to disrupt the *cntd1* gene in RCC and observed the resultant phenotype in the F0 generation. The efficient induction of germ cell mutations in F0 individuals, facilitated by Cas9 protein injection, played a crucial role in these findings. Specifically, male F0 RCC exhibited a marked decrease in sperm production, along with increased occurrence of spermatocyte arrest and apoptotic signals. In contrast, F0 female RCC displayed normal ovarian development and retained the ability to spawn and fertilize during the breeding season. This indicates a clear sexual dimorphism in the impact of *cntd1* knockout on reproductive development in RCC. Moreover, an intriguing outcome of this research was observed in some female F0 knockout fish, in which their progeny exhibited abnormal development and various ploidy levels. Despite these abnormalities, a subset of F1 offspring survived. Further analyses through flow cytometry assays, chromosome analysis, and morphological examination of erythrocytes confirmed that these surviving offspring comprised both diploid and triploid individuals. These findings, in conjunction with previous research on the *cntd1* gene in zebrafish (Ou et al., 2024), suggest a conserved role of *cntd1* in maintaining normal gametogenesis and its knockout in regulating ploidy in different fish species.

To date, triploids have primarily been produced through two methods: artificial induction and distant hybridization. The former involves inhibiting the extrusion of the second polar body through temperature or hydrostatic pressure shock, a method successfully applied across more than ten fish species (Felip et al., 2001; Hassan et al., 2018; Káldy and Patakiné Várkonyi, 2021; Nwachi and Esa, 2016; Oppedal et al., 2003; Swarup, 1959b). However, a recent study revealed chromosomal aberrations resulting from hydrostatic pressure induction in Atlantic salmon despite successful triploid formation. These aberrations are implicated in the suboptimal growth performance observed in artificially induced triploid salmon (Glover and Harvey, 2020), suggesting that artificial induction may introduce deleterious genetic variations. This hypothesis was supported by the findings of another study in which triploid hybrids were induced through heat shock treatment of fertilized eggs obtained from female zebrafish and male blunt snout bream, resulting in allotriploids resembling zebrafish (Fu et al., 2020), whereas non-induced allotriploids exhibited a blend of parental traits (Liu et al.,

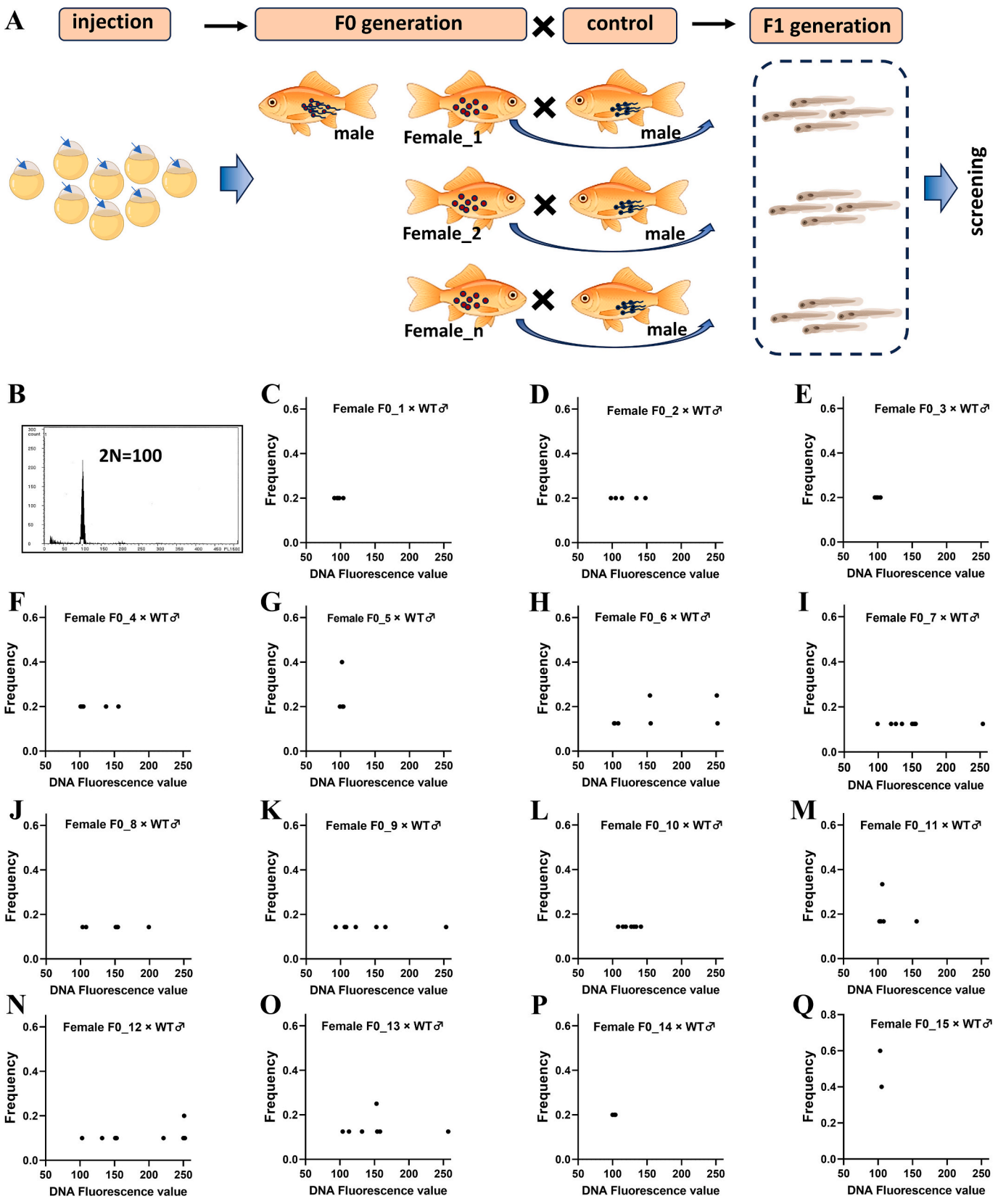

Fig. 3. Pre-screening of positive F0 females. A, Diagram of producing F1 embryos. B, The DNA content histogram of WT embryos. C-Q, Ploidy analysis of F1 embryos from each F0 female by flow cytometry. Ten embryos from each F0 female were collected as five samples.

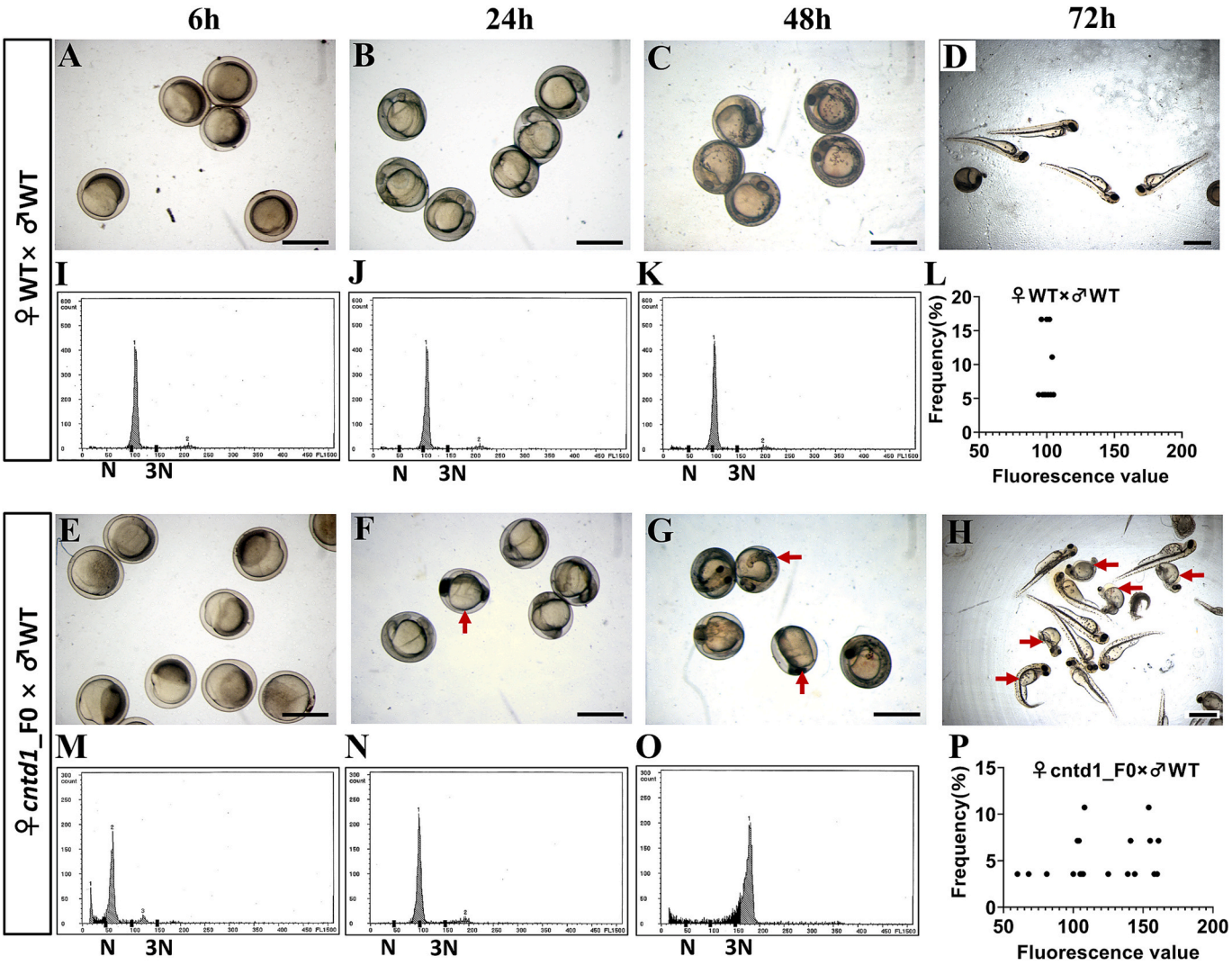

Fig. 4. Various deformities and ploidies existed in the F1 embryos. A-H, Observations of embryonic development in WT embryos (A-D) and embryos produced by positive *cntd1* knockout F0 females (*E*-F) at 6 h (A and E), 24 h (B and F), 48 h (C and G) and 72 h (D and H) post fertilization. The scale bar represents 1 mm. h, hour. I-K, Representative images of ploidy analysis by flow cytometry in WT embryos. L, Summary of ploidy results in WT embryos. M-O, Representative images of ploidy analysis by flow cytometry in embryos produced by positive *cntd1* knockout F0 females. P, Summary of ploidy results in embryos produced by positive *cntd1* knockout F0 females. For ploidy analysis, twenty embryos were collected as twenty samples.

2021a; Wang et al., 2022; Wang et al., 2021). These findings suggest that artificial induction may suppress gene or genome expression in polyploid fish. Distant hybridization represents an alternative important avenue for modifying fish ploidy. Our laboratory has focused on hybridization breeding in fish for more than three decades and has successfully established four polyploid strains (Wang et al., 2019). However, consistent patterns in regulating fish ploidy through hybridization have not emerged, as the ploidy of hybrid offspring varies across different species of fish. Therefore, the establishment of an allotetraploid strain may involve multiple generations of selection or one-step hybridization (Hu et al., 2019; Liu et al., 2001; Qin et al., 2014; Wang et al., 2020b). The mechanism underlying polyploidization via distant hybridization remains unclear, posing challenges for generating tetraploids across other fish species. In this study, we demonstrate that female RCCs with *cntd1* mutation acquire the ability to produce unreduced eggs and polyploid offspring, consistent with the observations in zebrafish (Ou et al., 2024). These findings suggest that the method of regulating offspring ploidy by controlling the parental *cntd1* genotype is applicable to a variety of fish species. In contrast to ploidy regulation via artificial induction and distant hybridization, the method developed in this study avoids the potential for deleterious genetic variation associated with artificial induction and exhibits broad applicability to a diverse range of fish species.

Meiotic processes exhibit significant sexual dimorphism during gametogenesis in mammals, where females and males differ notably in the regulation of cell cycle progression and dynamics (Handel and Eppig, 1998; Koehler et al., 2002). Studies utilizing mouse knockout models have revealed that mutations affecting synapsis or recombination typically result in defective reproductive development in males, contrasting with milder impacts on female fertility (Hua and Liu, 2021). For instance, mutations associated with chiasma formation render males completely sterile, whereas females generally maintain normal ovarian development but suffer from reduced fertility (Edelmann et al., 1996; Holloway et al., 2014). A greater tolerance of females to meiotic defects is also observed in fish (Feitsma et al., 2007; Ou et al., 2024; Zhang et al., 2020). Specifically, mutations affecting chiasma formation genes such as *mlh1* and *cntd1* induce severe inhibition of spermatogenesis in males, marked by spermatocyte developmental arrest and apoptosis, while females primarily exhibit altered egg ploidy without significantly compromising ovarian development or egg production (Feitsma et al., 2007; Ou et al., 2024). The differential tolerance to meiotic defects in chiasma formation likely arises from the distinct processes of

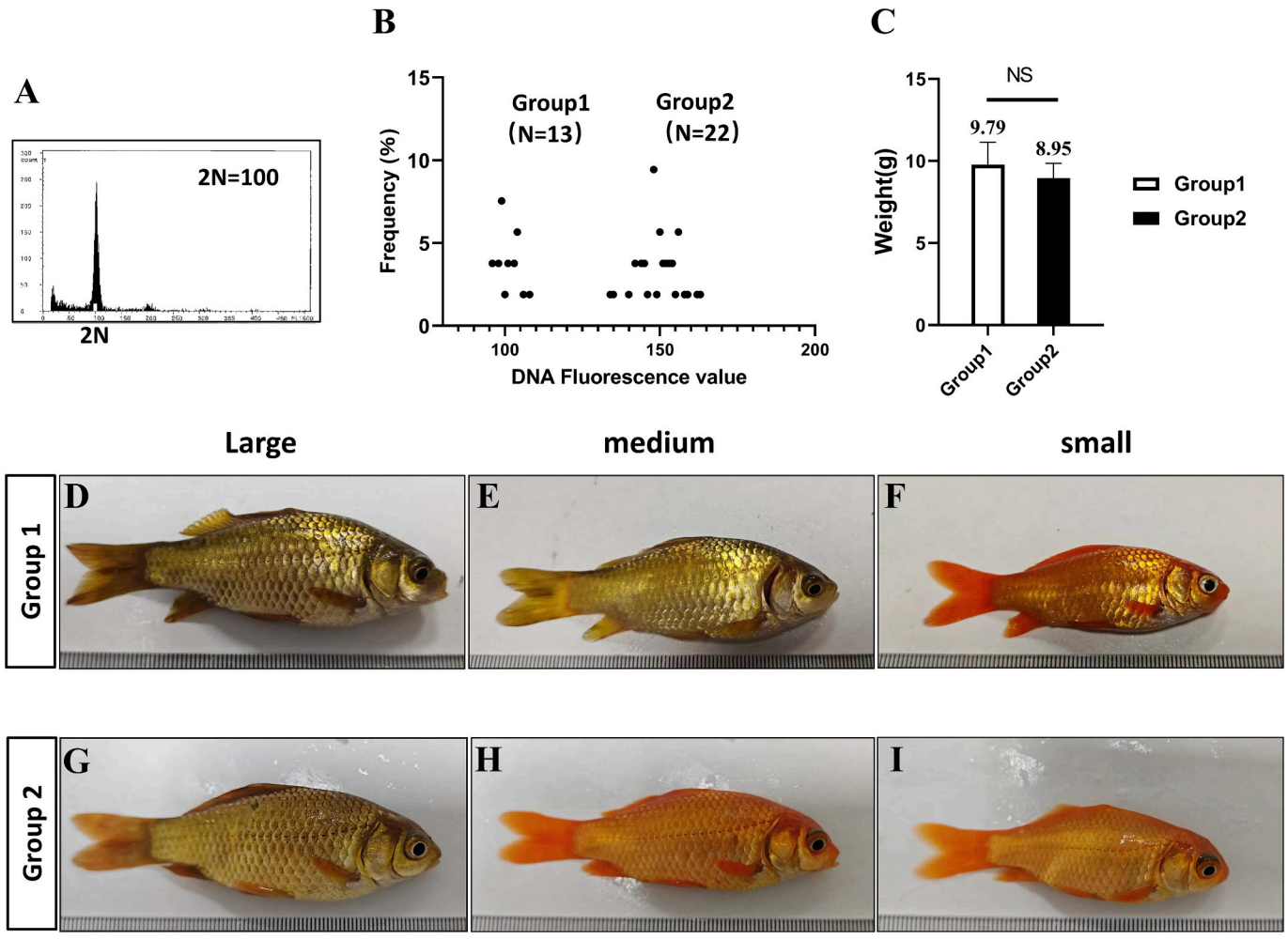

Fig. 5. Analysis of ploidy and body weights of the surviving F1 offspring. A, The DNA content histogram of WT individual. B, Ploidy analysis of the F1 offspring by flow cytometry. C, Weight analysis of the F1 offspring from different groups. The results are presented as mean ± standard error ($n \geq 3$). "NS" indicates no significant difference between two groups. D-I, Appearance of the F1 offspring from different groups in the range of large, medium, and small body size.

spermatogenesis and oogenesis. Male gametes complete meiosis in vivo across species, whereas oogenesis involves two cell cycle arrests, with the egg completing the second meiosis only upon fertilization (Kim et al., 2023; Masui and Markert, 1971; Yamashita, 1998). The first arrest occurs during prophase I of the first meiosis, allowing the egg to achieve full growth through yolk accumulation and the synthesis of maternally derived RNA and proteins. Subsequently, the egg matures, the first polar body is extruded, and the egg enters metaphase II of the second meiosis, at which point it arrests until fertilization (Yamashita, 1998). This sequence suggests that oocytes achieve full growth prior to encountering potential meiotic crossover defects, potentially explaining the greater resilience of females to such defects. In this study, we leveraged the resilience of female meiosis to crossover defects, demonstrating that these defects do not disrupt oogenesis but rather result in altered egg ploidy, leading to the production of triploid zygotes. However, the results of flow cytometry assays conducted at both the embryonic and adult stages indicate that the current yield of triploid RCC remains restricted in both proportion and quantity, and is not yet sufficiently efficient for practical application in aquaculture. Notably, our prior investigation in zebrafish suggested that tetraploid heterozygotes could arise from crosses between female homozygotes and control males. These tetraploid heterozygotes achieved stable strain status through successive self-breeding or facilitate the production of an entirely triploid cohort by mating with diploids (Ou et al., 2024). Given that Cntd1 depletion is also associated with the ability to generate unreduced eggs in RCC, it's reasonable to hypothesize that tetraploid RCC could be obtained from triploid homozygotes. Once tetraploid RCC are successfully produced, they have the potential to significantly improve the efficiency of triploid production, with the possibility of being applied in the aquaculture industry.

Growth performance serves as a crucial metric for evaluating the value of triploid fish; however, there remains ongoing discourse regarding their comparative growth rates. Some investigations have reported accelerated growth rates in triploid fish relative to their diploid counterparts (Afroz et al., 2021; Huang et al., 2023; Park et al., 2018). In contrast, other studies argue that artificially induced triploid fish do not exhibit a significant growth advantage (Benfey, 1999; Galbreath et al., 1994; McCarthy et al., 1996). The growth performance of triploids appears to be influenced by environmental conditions, with improved growth rates observed under isolated rearing conditions (Taylor et al., 2014). In this study, we found no discernible difference in growth performance between diploids and triploids in F1 offspring under identical culture conditions. This current finding lends partial support to the viewpoint that triploids exhibit a growth advantage only under isolated rearing conditions. However, further comparative breeding experiments between isolated and mixed rearing conditions are necessary for greater rigor. These findings suggest that the growth traits of triploids are influenced by both ploidy and culture pattern, highlighting the need to consider a combination of factors in commercial utilization.

Overall, we propose a novel approach for regulating RCC ploidy

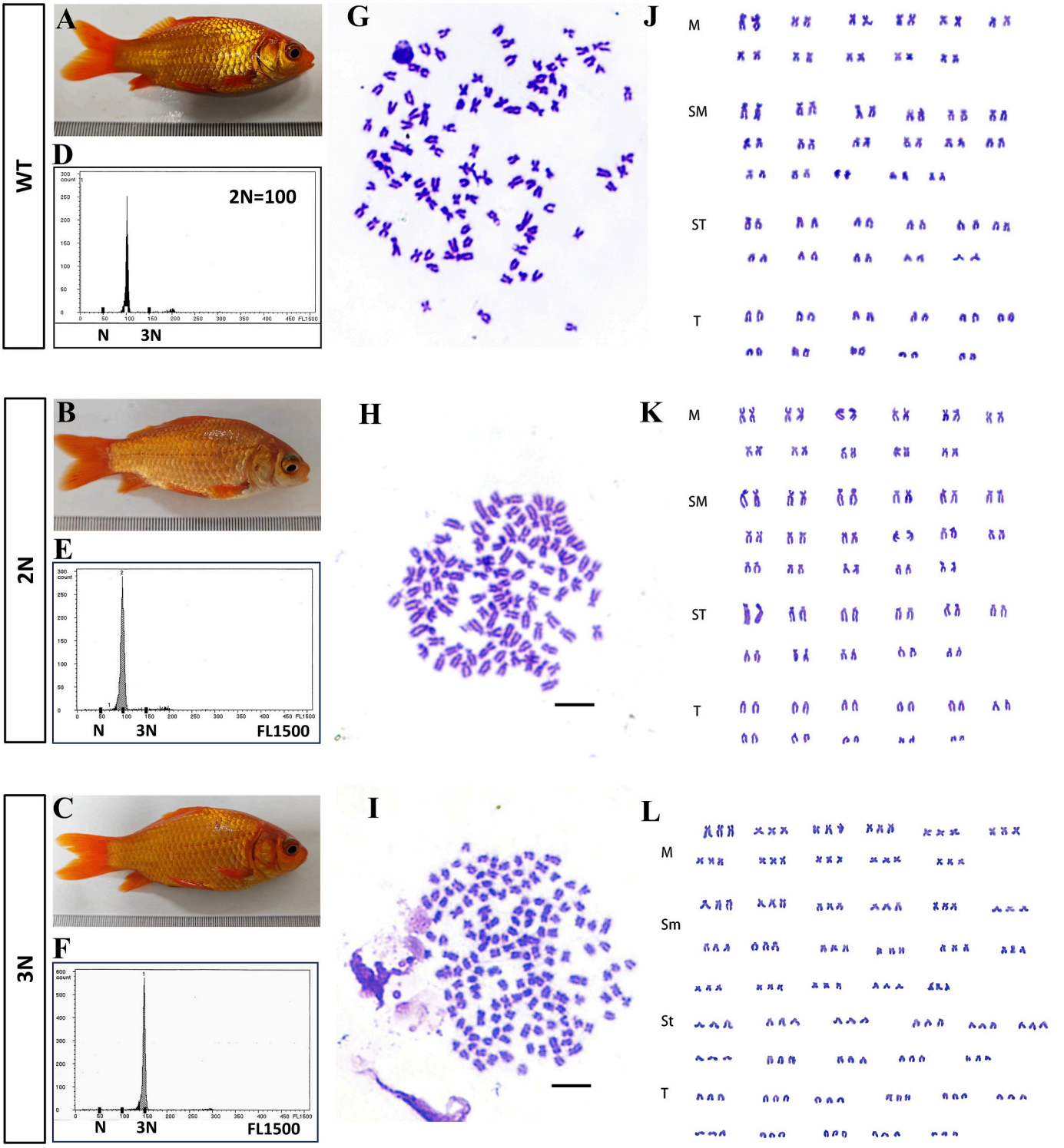

Fig. 6. Chromosome analysis of the F1 offspring. A-C, Representative images of WT RCC, diploid and triploid F1 offspring used for chromosome preparation. D-F, Representative results of DNA content in WT RCC, diploid and triploid F1 offspring. G-I, Chromosome analysis of WT RCC, diploid and triploid F1 offspring. The scale bar represents 5 μm. J-L, Chromosomal karyotype analysis of WT RCC, diploid and triploid F1 offspring.

through *cntd1* knockout, offering genetic control that avoids the reliance on artificial induction and hybridization pressures. This approach represents a substantial advancement in facilitating the breeding of polyploid fish.

5. Conclusion

In this study, the F0 generation of *cntd1* knockout RCC was generated using CRISPR/Cas9 technology. Male F0 RCC exhibited significant inhibition of spermatogenesis, marked by arrested spermatocytes at the metaphase of meiosis and increased apoptosis. Conversely, female F0 RCC experienced altered egg ploidy during oogenesis, resulting in F1

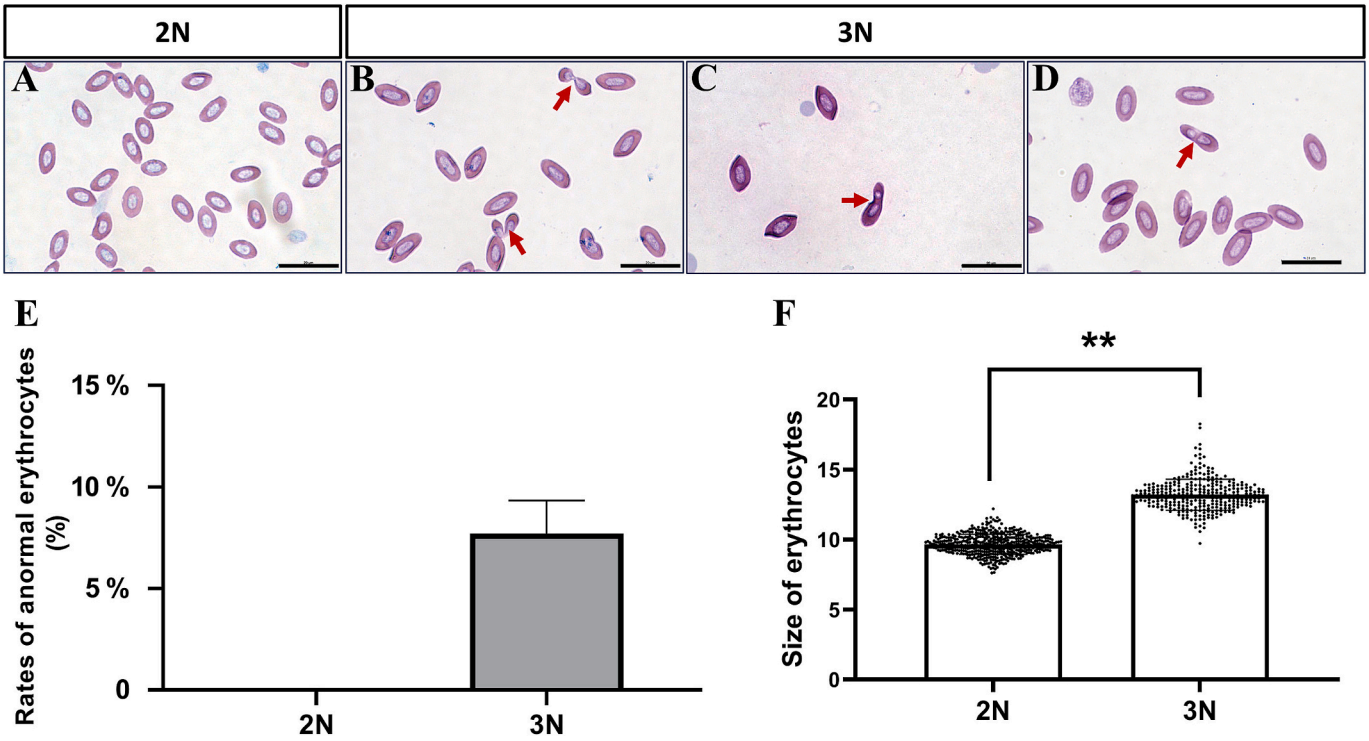

Fig. 7. Analysis of erythrocytic morphology in diploid and triploid offspring. A-D, Representative images of erythrocytes in diploid (A) and triploid (B-D) progenies. The scale bar represents 5 μm. E, Summary of the rates of abnormal erythrocytes in diploid and triploid progenies. F, Summary of the erythrocytic sizes in diploid and triploid progenies. 2 N represents diploids. 3 N represents triploids.

progeny with varying ploidy levels. Notably, only diploid and triploid F1 offspring survived to maturity. This research underscores the pivotal role of Cntd1 in governing reproductive development and ploidy maintenance in RCC, suggesting its potential as a target for genetic manipulation in aquaculture and evolutionary investigations.

Supplementary data to this article can be found online at https://doi.org/10.1016/j.aquaculture.2025.742347.

CRediT authorship contribution statement

Huilin Li: Writing – original draft, Methodology, Investigation, Formal analysis. **Yu Zhang:** Writing – review & editing, Methodology, Investigation, Formal analysis. **Lina Zhang:** Methodology, Investigation, Formal analysis. **Juan Li:** Methodology, Investigation, Formal analysis. **Yuan Ou:** Methodology, Investigation, Formal analysis. **Ming Wen:** Validation, Methodology, Conceptualization. **Zehong Wei:** Validation, Methodology, Conceptualization. **Jing Wang:** Validation, Methodology, Conceptualization. **Yu Deng:** Methodology. **Yinjun Jiang:** Methodology. **Conghui Yang:** Funding acquisition. **Yuqin Shu:** Writing – review & editing, Validation, Supervision, Resources, Methodology, Funding acquisition, Conceptualization. **Shaojun Liu:** Supervision, Resources.

Declaration of competing interest

The authors declare that they have no competing interests.

Acknowledgments

This work was supported by the National Natural Science Foundation of China (32293252, 32293251, 31802291, 32202912, 32473133) and the Natural Science Foundation of Hunan Province (2021JJ40342), Changsha Science and Technology Project (kq2402159).

Data availability

Data will be made available on request.

References

Afroz, K.B., Shah, M.S., Salin, K.R., Rahi, M.L., 2021. Growth and survival of diploid and triploid bata, Labeo bata (Hamilton, 1822). Aquaculture 1, 42–50. https://doi.org/10.1002/aff2.20.

Arai, K., 2001. Genetic improvement of aquaculture finfish species by chromosome manipulation techniques in Japan. Aquaculture 197, 205–228. https://doi.org/10.1016/S0044-8486(01)00588-9.

Baars, D.L., Takle, K.A., Heier, J., Pelegri, F., 2016. Ploidy manipulation of zebrafish embryos with heat shock 2 treatment. J. Vis. Exp. 16, 54492. https://doi.org/10.3791/54492.

Benfey, T.J., 1999. The physiology and behavior of triploid fishes. Rev. Fish. Sci. 7, 39–67. https://doi.org/10.1080/10641269991319162.

Benfey, T.J., 2001. Use of sterile triploid Atlantic salmon (*Salmo salar* L.) for aquaculture in New Brunswick, Canada. ICES J. Mar. Sci. 58, 525–529. https://doi.org/10.1006/jmsc.2000.1019.

Benfey, T.J., 2016. Effectiveness of triploidy as a management tool for reproductive containment of farmed fish: Atlantic salmon (*Salmo salar*) as a case study. Rev. Aquac. 8, 264–282. https://doi.org/10.1111/raq.12092.

Carrasco, L.A., Doroshov, S., Penman, D.J., Bromage, N., 1998. Long-term, quantitative analysis of gametogenesis in autotriploid rainbow trout, *Oncorhynchus mykiss*. J. Reprod. Infertil. 113, 197–210. https://doi.org/10.1530/jrf.0.1130197.

Chen, S., Wang, J., Liu, S., Qin, Q., Xiao, J., Duan, W., Luo, K., Liu, J., Liu, Y., 2009. Biological characteristics of an improved triploid crucian carp. Sci. China Life Sci. 52, 733–738. https://doi.org/10.1007/s11427-009-0079-3.

Chourrout, D., Chevassus, B., Krieg, F., Happe, A., Burger, G., Renard, P., 1986. Production of second generation triploid and tetraploid rainbow trout by mating tetraploid males and diploid females — potential of tetraploid fish. Theor. Appl. Genet. 72, 193–206. https://doi.org/10.1007/BF00266992.

Cotter, D., O'Donovan, V., O'Maoiléidigh, N., Rogan, G., Roche, N., Wilkins, N.P., 2000. An evaluation of the use of triploid Atlantic salmon (*Salmo salar* L.) in minimising the impact of escaped farmed salmon on wild populations. Aquaculture 186, 61–75. https://doi.org/10.1016/S0044-8486(99)00367-1.

Edelmann, W., Cohen, P.E., Kane, M., Lau, K., Morrow, B., Bennett, S., Umar, A., Kunkel, T., Cattoretti, G., Chaganti, R., Pollard, J.W., Kolodner, R.D., Kucherlapati, R., 1996. Meiotic pachytene arrest in MLH1-deficient mice. Cell 85, 1125–1134. https://doi.org/10.1016/s0092-8674(00)81312-4.

Feitsma, H., Leal, M.C., Moens, P.B., Cuppen, E., Schulz, R.W., 2007. Mlh1 deficiency in zebrafish results in male sterility and aneuploid as well as triploid progeny in females. Genetics 175, 1561–1569. https://doi.org/10.1534/genetics.106.068171.

Felip, A., Zanuy, S., Carrillo, M., Piferrer, F., 2001. Induction of triploidy and gynogenesis in teleost fish with emphasis on marine species. Genetica 111, 175–195. https://doi.org/10.1023/A:1013724322169.

Fu, W., Peng, L., Wu, X., He, S., Zhao, H., Liu, J., Liu, W., Xiao, Y., 2020. Triploidization of hybrids (female zebrafish × male blunt snout bream) by heat-shock can improve survival rate. Aquaculture 517, 734786. https://doi.org/10.1016/j.aquaculture.2019.734786.

Galbreath, P.F., Jean, W.S., Anderson, V., Thorgaard, G.H., 1994. Freshwater performance of all-female diploid and triploid Atlantic salmon. Aquaculture 128, 41–49. https://doi.org/10.1016/0044-8486(94)90100-7.

Glover, K.A., Harvey, A.C., 2020. Chromosome aberrations in pressure-induced triploid Atlantic salmon. BMC Genomics 21, 59. https://doi.org/10.1186/s12863-020-00864-0.

Goo, I.B., Im, J.H., Gil, H.W., Lim, S.G., Park, I.S., 2015. Comparison of cell and nuclear size difference between diploid and induced triploid in marine medaka, *Oryzias dancena*. Dev. Reprod. 19, 127–134. https://doi.org/10.12717/dr.2015.19.3.127.

Güralp, H., Skaftnesmo, K.O., Kjærner-Semb, E., Straume, A.H., Kleppe, L., Schulz, R.W., Edvardsen, R.B., Wargelius, A., 2020. Rescue of germ cells in dnd crispant embryos opens the possibility to produce inherited sterility in Atlantic salmon. Sci. Rep. 10, 18042. https://doi.org/10.1038/s41598-020-74876-2.

Handel, M.A., Eppig, J.J., 1998. Sexual dimorphism in the regulation of mammalian meiosis. Curr. Top. Dev. Biol. 37, 333–358. https://doi.org/10.1016/S0070-2153(08)60179-9.

Hassan, A., Okomoda, V.T., Sanusi, F.A.B., 2018. Fertilization, hatching, and embryogenesis of diploid and triploid eggs of *Anabas testudineus* (Bloch, 1792). Zygote 26, 343–349. https://doi.org/10.1017/s0967199418000187.

Holloway, J.K., Sun, X., Yokoo, R., Villeneuve, A.M., Cohen, P.E., 2014. Mammalian CNTD1 is critical for meiotic crossover maturation and deselection of excess precrossover sites. J. Cell Biol. 205, 633–641. https://doi.org/10.1083/jcb.201401122.

Hu, F., Fan, J., Qin, Q., Huo, Y., Wang, Y., Wu, C., Liu, Q., Li, W., Chen, X., Liu, C., Tao, M., Wang, S., Zhao, R., Luo, K., Liu, S., 2019. The sterility of allotriploid fish and fertility of female autotriploid fish. Front. Genet. 10, 377. https://doi.org/10.3389/fgene.2019.00377.

Hua, R., Liu, M., 2021. Sexual dimorphism in mouse meiosis. Front. Cell Dev. Biol. 9, 670599. https://doi.org/10.3389/fcell.2021.670599.

Huang, Z., Dai, L., Peng, F., Tang, L., Wang, X., Chen, J., Liu, J., Fu, W., Peng, L., Liu, W., Xiao, Y., 2023. mTOR signaling pathway regulates embryonic development and rapid growth of triploid crucian carp. Aquacult. Rep. 33, 101860. https://doi.org/10.1016/j.aqrep.2023.101860.

Ju, R.-T., Li, X., Jiang, J.-J., Wu, J., Liu, J., Strong, D.R., Li, B., 2020. Emerging risks of non-native species escapes from aquaculture: call for policy improvements in China and other developing countries. J. Appl. Ecol. 57, 85–90. https://doi.org/10.1111/1365-2664.13521.

Káldy, J., Patakiné Várkonyi, E., 2021. Effects of hydrostatic pressure treatment of newly fertilized eggs on the ploidy level and karyotype of pikeperch *Sander lucioperca* (Linnaeus, 1758). Life (Basel) 11, 1296. https://doi.org/10.3390/life11121296.

Kim, H.M., Kang, M.K., Seong, S.Y., Jo, J.H., Kim, M.J., Shin, E.K., Lee, C.G., 2023. Meiotic cell cycle progression in mouse oocytes: role of cyclins. Int. J. Mol. Sci. 24, 13659. https://doi.org/10.3390/ijms241713659.

Koehler, K.E., Millie, E.A., Cherry, J.P., Burgoyne, P.S., Evans, E.P., Hunt, P.A., Hassold, T.J., 2002. Sex-specific differences in meiotic chromosome segregation revealed by dicentric bridge resolution in mice. Genetics 162, 1367–1379.

Lahnsteiner, F., Kletzl, M., 2018. Pressure shock triploidization of *Salmo trutta f. lacustris* and *Salvelinus umbla* eggs and its impact on fish development. Theriogenology 115, 65–76. https://doi.org/10.1016/j.theriogenology.2018.04.020.

Lebeda, I., Flajshans, M., 2015. Technical note: production of tetraploid sturgeons. J. Anim. Sci. 93, 3759–3764. https://doi.org/10.2527/jas.2015-9094.

Liu, S., Liu, Y., Zhou, G., Zhang, X., Luo, C., Feng, H., He, X., Zhu, G., Yang, H., 2001. The formation of tetraploid stocks of red crucian carp×common carp hybrids as an effect of interspecific hybridization. Aquaculture 192, 171–186. https://doi.org/10.1016/S0044-8486(00)00451-8.

Liu, W., Wen, Y., Wang, M., Gui, S., Li, X., Fan, Y., Yan, X., Lin, Y., Sun, Y., Liu, J., Peng, L., Liu, S., Li, D.W., Xiao, Y., 2018. Enhanced resistance of triploid crucian carp to cadmiuminduced oxidative and endoplasmic reticulum stresses. Curr. Mol. Med. 18, 400–408. https://doi.org/10.2174/1566524018666181113105018.

Liu, Q., Zhang, X., Liu, J., Liu, F., Shi, F., Qin, Q., Tao, M., Tang, C., Liu, S., 2021a. A new type of allodiploid hybrids derived from female *Megalobrama amblycephala* × male *Gobiocypris rarus*. Front. Genet. 12, 685914. https://doi.org/10.3389/fgene.2021.685914.

Liu, W.B., Wang, M.M., Dai, L.Y., Dong, S.H., Yuan, X.D., Yuan, S.L., Tang, Y., Liu, J.H., Peng, L.Y., Xiao, Y.M., 2021b. Enhanced immune response improves resistance to cadmium stress in triploid crucian carp. Front. Physiol. 12, 666363. https://doi.org/10.3389/fphys.2021.666363.

Martins, L.F., Hilbig, C.C., Yasui, G.S., Monzani, P.S., Senhorini, J.A., 2021. Return temperature after heat shock affects the production of tetraploids in the yellowtail tetra *Astyanax altiparanae*. Zygote 29, 82–86. https://doi.org/10.1017/s096719942000043x.

Masui, Y., Markert, C.L., 1971. Cytoplasmic control of nuclear behavior during meiotic maturation of frog oocytes. J. Exp. Zool. 177, 129–145. https://doi.org/10.1002/jez.1401770202.

McCarthy, I.D., Carter, C.G., Houlihan, D.F., Johnstone, R., Mitchell, A.I., 1996. The performance of all-female diploid and triploid Atlantic salmon smolts on transfer together to sea water. J. Fish Biol. 48, 545–548. https://doi.org/10.1111/j.1095-8649.1996.tb01448.x.

Nam, Y.K., Choi, G.C., Kim, D.S., 2004. An efficient method for blocking the 1st mitotic cleavage of fish zygote using combined thermal treatment, exemplified by mud loach (*Misgurnus mizolepis*). Theriogenology 61, 933–945. https://doi.org/10.1016/s0093-691x(03)00258-9.

Nwachi, O.F., Esa, Y.B., 2016. Comparative growth and survival of diploid and triploid Mozambique tilapia (*Oreochromism ossambicus*) reared in indoor tanks. J. Environ. Biol. 37, 839–843.

Oppedal, F., Taranger, G.L., Hansen, T., 2003. Growth performance and sexual maturation in diploid and triploid Atlantic salmon (*Salmo salar* L.) in seawater tanks exposed to continuous light or simulated natural photoperiod. Aquaculture 215, 145–162. https://doi.org/10.1016/S0044-8486(02)00223-5.

Ou, Y., Li, H., Li, J., Dai, X., He, J., Wang, S., Liu, Q., Yang, C., Wang, J., Zhao, R., Yin, Z., Shu, Y., 2024. Formation of different polyploids through disrupting meiotic crossover frequencies based on cntd1 knockout in zebrafish. Mol. Biol. Evol. 41, msae047. https://doi.org/10.1093/molbev/msae047.

Park, I.S., Gil, H.W., Kim, D.S., 2018. Morphometric characteristics of diploid and triploid marine medaka, *Oryzias dancena*. Dev. Reprod. 22, 183–192. https://doi.org/10.12717/dr.2018.22.2.183.

Peruzzi, S., Chatain, B., 2003. Induction of tetraploid gynogenesis in the european sea bass (*Dicentrarchus labrax* L.). Genetica 119, 225–228. https://doi.org/10.1023/A:1026077405294.

Piferrer, F., Beaumont, A., Falguière, J.-C., Flajšhans, M., Haffray, P., Colombo, L., 2009. Polyploid fish and shellfish: production, biology and applications to aquaculture for performance improvement and genetic containment. Aquaculture 293, 125–156. https://doi.org/10.1016/j.aquaculture.2009.04.036.

Qin, Q., Wang, Y., Wang, J., Dai, J., Xiao, J., Hu, F., Luo, K., Tao, M., Zhang, C., Liu, Y., Liu, S., 2014. The autotetraploid fish derived from hybridization of *Carassius auratus* red var. (female) × *Megalobrama amblycephala* (male). Biol. Reprod. 91, 93. https://doi.org/10.1095/biolreprod.114.122283.

Ren, L., Zhang, H., Luo, M., Gao, X., Cui, J., Zhang, X., Liu, S., 2022. Heterosis of growth trait regulated by DNA methylation and miRNA in allotriploid fish. Epigenetics Chromatin 15, 19. https://doi.org/10.1186/s13072-022-00455-6.

Swarup, H., 1959a. Effect of triploidy on the body size, general organization and cellular structure in *Gasterosteus aculeatus* (L). J. Genet. 56, 143–155. https://doi.org/10.1007/BF02984741.

Swarup, H., 1959b. Production of triploidy in *Gasterosteus aculeatus* (L). J. Genet. 56, 129–142. https://doi.org/10.1007/BF02984740.

Taylor, J.F., Bozzolla, P., Frenzl, B., Matthew, C., Hunter, D., Migaud, H., 2014. Triploid Atlantic salmon growth is negatively affected by communal ploidy rearing during seawater grow-out in tanks. Aquaculture 432, 163–174. https://doi.org/10.1016/j.aquaculture.2014.05.014.

Wang, S., Tang, C., Tao, M., Qin, Q., Zhang, C., Luo, K., Zhao, R., Wang, J., Ren, L., Xiao, J., Hu, F., Zhou, R., Duan, W., Liu, S., 2019. Establishment and application of distant hybridization technology in fish. Sci. China Life Sci. 62, 22–45. https://doi.org/10.1007/s11427-018-9408-x.

Wang, S., Xu, X., Luo, K., Liu, Q., Chen, L., Wei, Z., Zhou, P., Hu, F., Liu, Z., Tao, M., Liu, S., 2020a. Two new types of triploid hybrids derived from *Cyprinus carpio* (♀) × *Megalobrama amblycephala* (♂). Aquaculture 528, 735448. https://doi.org/10.1016/j.aquaculture.2020.735448.

Wang, S., Zhou, P., Huang, X., Liu, Q., Lin, B., Fu, Y., Gu, Q., Hu, F., Luo, K., Zhang, C., Tao, M., Qin, Q., Liu, S., 2020b. The establishment of an autotetraploid fish lineage produced by female allotetraploid hybrids × male homodiploid hybrids derived from *Cyprinus carpio* (♀) × *Megalobrama amblycephala* (♂). Aquaculture 515, 734583. https://doi.org/10.1016/j.aquaculture.2019.734583.

Wang, Y., Yao, J., Luo, Y., Tan, H., Huang, X., Wang, S., Qin, Q., Zhang, C., Tao, M., Dabrowski, K., Liu, S., 2021. Two new types of homodiploid fish and polyploid hybrids derived from the distant hybridization of female koi carp and male bighead carp. Mar. Biotechnol. 23, 628–640. https://doi.org/10.1007/s10126-021-10050-7.

Wang, J., He, W., Wang, W., Luo, Z., Han, L., Xiang, C., Chai, M., Li, T., Li, J., Luo, K., Zhao, R., Liu, S., 2022. A novel allotriploid hybrid derived from female goldfish × male Bleeker's yellow tail. Front. Genet. 13, 880591. https://doi.org/10.3389/fgene.2022.880591.

Wang, M., Ou, Y., Guo, Z., Li, J., Li, H., Li, X., Li, J., Wang, S., Liu, Q., Wang, J., Shu, Y., Liu, S., 2024. Characterization of allodiploid and allotriploid fish derived from hybridization between *Cyprinus carpio haematopterus* (♀) and *Gobiocypris rarus* (♂). Reprod. Breed. 4, 46–54. https://doi.org/10.1016/j.repbre.2023.12.005.

Wargelius, A., Leininger, S., Skaftnesmo, K.O., Kleppe, L., Andersson, E., Taranger, G.L., Schulz, R.W., Edvardsen, R.B., 2016. Dnd knockout ablates germ cells and demonstrates germ cell independent sex differentiation in Atlantic salmon. Sci. Rep. 6, 21284. https://doi.org/10.1038/srep21284.

Wong, T.T., Zohar, Y., 2015. Production of reproductively sterile fish: a mini-review of germ cell elimination technologies. Gen. Comp. Endocrinol. 221, 3–8. https://doi.org/10.1016/j.ygcen.2014.12.012.

Yamashita, M., 1998. Molecular mechanisms of meiotic maturation and arrest in fish and amphibian oocytes. Semin. Cell Dev. Biol. 9, 569–579. https://doi.org/10.1006/scdb.1998.0251.

Yang, Z., Yu, Y., Tay, Y.X., Yue, G.H., 2022. Genome editing and its applications in genetic improvement in aquaculture. Rev. Aquac. 14, 178–191. https://doi.org/10.1111/raq.12591.

Yokoo, R., Zawadzki, K.A., Nabeshima, K., Drake, M., Arur, S., VilleneuveAM., 2012. COSA-1 reveals robust homeostasis and separable licensing and reinforcement steps governing meiotic crossovers. Cell 149 (1), 75–87. https://doi.org/10.1016/j.cell.2012.01.052.

Zhang, Y., Li, Z., Nie, Y., Ou, G., Chen, C., Cai, S., Liu, L., Yang, P., 2020. Sexually dimorphic reproductive defects in zebrafish with spo11 mutation. Aquac. Res. 51, 4916–4924. https://doi.org/10.1111/are.14829.

Zhang, C., Li, Q., Zhu, L., He, W., Yang, C., Zhang, H., Sun, Y., Zhou, L., Sun, Y., Zhu, S., Wu, C., Tao, M., Zhou, Y., Zhao, R., Tang, C., Liu, S., 2021. Abnormal meiosis in fertile and sterile triploid cyprinid fish. Sci. China Life Sci. 64, 1917–1928. https://doi.org/10.1007/s11427-020-1900-7.

Zhu, X., Lin, Z., Wu, Z., Li, J., You, F., 2017. Effect of initiation time of hydrostatic pressure shock on chromosome set doubling of tetraploidization in turbot *Scophthalmus maximus*. Mar. Biotechnol. 19, 528–540. https://doi.org/10.1007/s10126-017-9771-7.